AIP | Journal of Applied Physics

On the stochastic nature of resistive switching in Cu doped Ge0.3Se0.7 based memory devices

R. Soni, P. Meuffels, G. Staikov, R. Weng, C. Kügeler et al.

Citation: J. Appl. Phys. **110**, 054509 (2011); doi: 10.1063/1.3631013
View online: http://dx.doi.org/10.1063/1.3631013
View Table of Contents: http://jap.aip.org/resource/1/JAPIAU/v110/i5
Published by the American Institute of Physics.

On the stochastic nature of resistive switching in Cu doped $Ge_{0.3}Se_{0.7}$ based memory devices

R. Soni,[1] P. Meuffels,[1,a)] G. Staikov,[1,b)] R. Weng,[1] C. Kügeler,[2] A. Petraru,[3] M. Hambe,[3] R. Waser,[1] and H. Kohlstedt[3,c)]
[1]*Institut für Festkörperforschung, Forschungszentrum Jülich GmbH, Jülich, 52425, Germany*
[2]*Fraunhofer-IFAM, 26129, Oldenburg, Germany*
[3]*Nanoelektronik, Technische Fakultät Kiel, Christian-Albrechts-Universität Kiel, Kiel, 24143, Germany*

(Received 15 April 2011; accepted 25 July 2011; published online 9 September 2011)

Currently, there is great interest in using solid electrolytes to develop resistive switching based nonvolatile memories (RRAM) and logic devices. Despite recent progress, our understanding of the microscopic origin of the switching process and its stochastic behavior is still limited. In order to understand this behavior, we present a statistical "breakdown" analysis performed on Cu doped $Ge_{0.3}Se_{0.7}$ based memory devices under elevated temperature and constant voltage stress conditions. Following the approach of electrochemical phase formation, the precursor of the "ON resistance switching" is considered to be nucleation — the emergence of small clusters of atoms carrying the basic properties of the new phase which forms the conducting filament. Within the framework of nucleation theory, the observed fluctuations in the time required for "ON resistance switching" are found to be consistent with the stochastic nature of critical nucleus formation.
 [doi:10.1063/1.3631013]

I. INTRODUCTION

Resistive switching phenomena triggered by electrical stimulus have attracted a lot of attention due to potential non-volatile memory device applications. In recent years, an enormous range of materials in metal-insulator-metal configurations has been reported to show hysteretic resistance switching behavior.[1–14] Attractive properties of resistive switching memory devices, commonly known as resistive random access memory (RRAM), are low fabrication costs, scalability into the nanometer regime, fast write and read access, low power consumption and low threshold voltages.[15]

Solid electrolyte materials such as Ag and Cu doped amorphous Ge-Se (Ref. 16), Ge-S (Ref. 17) and (Zn, Cd)S (Ref. 18) as well as oxide thin films such as SiO_2 (Ref. 19) are some of the most promising candidates in the race for future RRAM cells. The macroscopic origin of the resistive switching phenomena in these material systems, when sandwiched between an electrochemically active metal, such as Ag, Cu, or Ni, and an electrochemically inert counter electrode, such as Pt, Ir, or Au, is reasonably well understood. It is proposed that the electrochemical formation and rupture of metallic filaments which are composed of the active metal and bridge the electrodes are responsible for the resistive switching effect.[15]

In recent years, much scientific knowledge has been gained on the basic ingredients of the resistive switching effect in these material systems and a lot of promising results have been reported.[12–14] However, the emergence of macroscopic switching effects from local microscopic events, the role of disorder during the switching process and the stochastic fluctuations in device performance are some of the open questions which need still to be addressed prior to industrial qualification.

There are mainly two crucial tasks in understanding the physics of resistive switching memory devices which are based upon these disordered material systems. First, the filament formation in the resistive switching process is a dynamic one by nature. In order to understand this process one must understand both the threshold conditions that trigger this process and the kinetics with which it proceeds. Second, one has to identify a model, necessary to elucidate the microscopic mechanisms underlying the macroscopic behavior. A simple approach in this case would be to match known information on the temperature and voltage dependence of the memory device characteristics to the physical parameters of a microscopic model.

In the past couple of decades, considerable efforts have been undertaken to investigate breakdown phenomena in solid materials under constant or dynamical stress conditions because of their importance in semiconductor industry for device reliability predictions.[20–24] When measuring the breakdown fields in dynamic tests or the "time-to-breakdown" in static tests, a statistical distribution is generally found. The breakdown statistics are usually related in some way to underlying random microscopic physical processes. Thus, studies on breakdown statistics may help to understand both the threshold conditions that trigger these processes as well as the responsible dynamical physical effects.

In this context, the initial idea for the present paper is straightforward. We have investigated the "breakdown" behavior, i.e., "ON resistance switching" from the high resistance (HRS) to the low resistance state (LRS), of Cu doped $Ge_{0.3}Se_{0.7}$ based memory devices under constant

a)Electronic mail: p.meuffels@fz-juelich.de.
b)Electronic mail: g.staikov@fz-juelich.de.
c)Electronic mail: hko@tf.uni-kiel.de.

voltage stress conditions (the term "breakdown" in the following test serves as a short synonym for "ON resistance switching from HRS to LRS"). Memory cells with different active areas and integrated $Ge_{0.3}Se_{0.7}$ thin film thicknesses in the HRS were measured at room temperature as well as at elevated temperatures and the statistical distributions of the measured "time-to-breakdown" were determined in order to get an insight into the microscopic resistive switching mechanisms and its stochastic nature.

II. EXPERIMENTAL

The memory cells were fabricated as planar capacitor structures with $Ge_{0.3}Se_{0.7}$ active layer thicknesses ranging from 30 to 120 nm and with areas ranging from 50×50 to 400×400 μm^2. Si (100) wafers with a 400 nm thermal oxide and a 5 nm TiO_2 film as an adhesion layer for the Pt base electrode deposition were used as substrates. A 30 nm thin film of Pt was sputtered on top and this bottom Pt electrode was patterned by standard optical lithography and by reactive ion beam etching (RIBE). The photoresist was removed with acetone and a buffer layer of 2 −3 nm SiO_x was deposited by radio frequency (RF) sputtering at a rate of 0.8 nm s^{-1} followed by defining the bottom electrode contact with optical lithography and RIBE. Afterwards, the top structure of the memory cell was defined by a lift-off step. The $Ge_{0.3}Se_{0.7}$ layers were deposited by RF-sputtering followed by the deposition of the 150 nm Cu top electrode. The deposition rates for the $Ge_{0.3}Se_{0.7}$ and Cu layers were around 0.2 and 0.5 nm s^{-1}, respectively. Finally, a lift-off in acetone was used to finalize the device structure. A schematic of a planar structure memory device is shown in Fig. 1(a). It is important to point out that no additional process such as UV photo or thermal assisted "annealing" was required to diffuse the copper ions into the $Ge_{0.3}Se_{0.7}$ layers. We have omitted such a treatment because, even at room temperature, copper

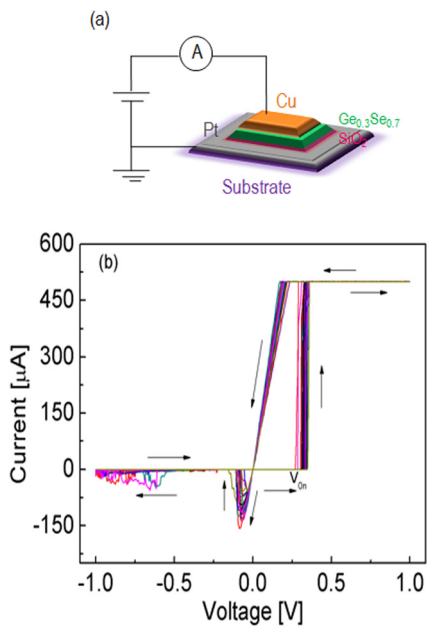

FIG. 1. (Color online) (a) Schematic of planar structure memory devices. (b) Typical *I-V* characteristics of a memory cell measured at room temperature with a 500 μA compliance current setting.

dissolves easily in amorphous germanium chalcogenide films of micrometer thickness without the support of UV photo or thermal assisted "annealing" processes.[25] However, there is no doubt that these processes are widely used to enhance the diffusion process.

The very thin SiO_x buffer layer "with expected pinholes" was introduced between the Cu-Ge-Se layer and the Pt bottom electrode to improve the switching characteristics and to achieve very low leakage currents. Figure 1(b) shows typical *I-V* characteristics of a dual layered memory cell measured at room temperature with a 500 μA current compliance setting. We observed that the "switch on" voltage V_{on} varied stochastically from cycle to cycle. More details on the resistive switching properties of these memory devices can be found in Refs. 26 and 27.

In order to understand these fluctuations in performance, we carried through a breakdown analysis by monitoring the current change of memory cells under constant voltage stress conditions. All measurements were done using an Agilent B1500 semiconductor parameter analyzer. To be able to observe the breakdown within a reasonable time, the stressing voltage was chosen to be equal to or smaller than the threshold "switch on" voltage V_{on}.

Figure 2 shows some typical examples of the breakdown behavior of memory cells with a $Ge_{0.3}Se_{0.7}$ active layer thickness of 90 nm and a 50×50 μm^2 cross-sectional area under constant voltage stress of 200 mV at room temperature. As can be seen, the elapsed times before the final breakdowns (HRS→LRS) varied considerably from device to device under the same stress conditions indicating that the underlying breakdown process is of stochastic nature. Similarly, this stochastic behavior was also observed for prebreakdown events before the final breakdown.

These preliminary results indicate that a statistical analysis is important to understand the nature of the breakdown process. Before going ahead with an analysis of the "time-to-breakdown" distributions or switching statistics, it is important to consider the various electrochemical processes involved in the "ON resistance switching from HRS to LRS" of Cu doped $Ge_{0.3}Se_{0.7}$ based memory cells.

III. PROCESSES INVOLVED IN THE RESISTIVE SWITCHING OF Cu DOPED $Ge_{0.3}Se_{0.7}$ BASED MEMORY CELLS

Under sufficient positive bias applied to the active Cu electrode, the resistance switching "ON process" involves the following steps:[15]

(1) anodic dissolution of Cu according to the reaction

$$Cu \rightarrow Cu^{z+} + ze^{-}, \quad (1)$$

where Cu^{z+} represents Cu cations with valence number z (Cu^{+} or Cu^{2+}) in the Cu doped $Ge_{0.3}Se_{0.7}$ thin film;

(2) migration of the Cu^{z+} cations across the thin film under the action of the applied electric field;

(3) reduction and electrocrystallization of Cu on the surface of the inert Pt electrode according to the cathodic deposition reaction

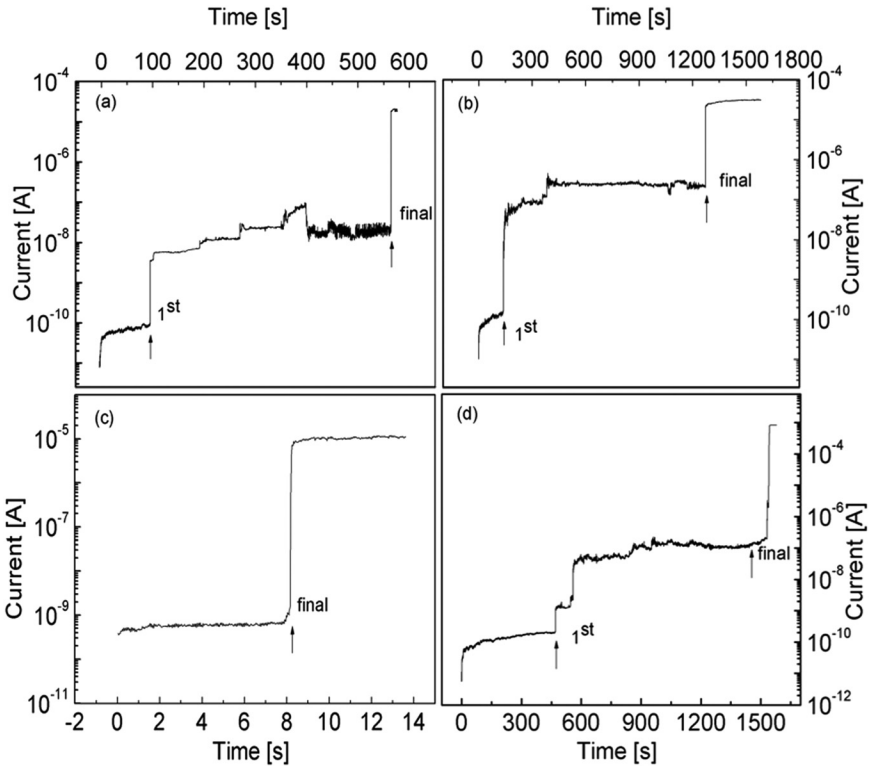

FIG. 2. (a)–(d) Resistance evolution of different memory cells, integrated with a 90 nm $Ge_{0.3}Se_{0.7}$ thin film, under a constant voltage stress of 200 mV at room temperature.

$$Cu^{z+} + ze^- \rightarrow Cu. \quad (2)$$

In order to identify the most probable process that accounts (i) for the statistical distribution of the time dependent breakdown events and (ii) for the characteristic switching times of the memory devices, these processes are discussed below.

The rate of migration of Cu^{z+} cations across the thin $Ge_{0.3}Se_{0.7}$-Cu film is determined by the cation mobility μ_{Cuz+} and the applied electric field E.[28–30] It is known that Ag or Cu doped chalcogenide materials (such as $Ge_{0.3}Se_{0.7}$) are good ionic conductors, exhibiting a cation mobility of the order of 10^{-2} to 10^{-4} cm^2/Vs.[31] The time τ_{mig} needed for a Cu^{z+} ion to migrate across a $Ge_{0.3}Se_{0.7}$-Cu film with thickness L can be roughly estimated using the relation $\tau_{mig} = L/\mu_{Cuz+}E$. With $\mu_{Cuz+} = 10^{-3}$ cm^2/Vs, $L = 100$ nm and an applied voltage of 200 mV, we estimate τ_{mig} to be of the order of <1 μs. If one considers a field dependent ion mobility which increases with increasing electric field strength at very high local fields,[29] τ_{mig} will further decrease. As we were working at time scales ≥ 1 ms in the present study, this leaves the ion migration [step (2)] out of discussion for the rate limiting step for the breakdown process in the investigated system.

Let us now consider the electrode reactions involving transfer of Cu^{z+} across both electrode/electrolyte interfaces. The current density for the charge transfer across the electrode/electrolyte interface during the anodic oxidation and dissolution of metal ions in the electrolyte, step (1), and the counter reaction representing the cathodic reduction leading to the metal deposition (i.e., electrocrystallization process) at the inert electrode, step (3), can generally be described by the Butler-Volmer equation:[32]

$$i = i_0\left[\exp\left(\frac{\alpha ze\eta}{k_BT}\right) - \exp\left(-\frac{(1-\alpha)ze\eta}{k_BT}\right)\right], \quad (3)$$

where i_0 is the exchange current density, α is the cathodic charge transfer coefficient and η represents the electrochemical overpotential defined as a difference between the equilibrium Nernst-potential φ_{eq} of the metal M and the actual electrode potential φ ($\eta = \varphi_{eq} - \varphi > 0$). k_B, T and e have their usual meanings.

For high cathodic overpotentials ($\eta \gg k_BT/ze$) Eq. (3) transforms to

$$\ln i = \frac{\alpha ze}{k_BT}\eta + \ln i_0. \quad (3a)$$

This logarithmic relationship between i and η can be used for an experimental determination of the charge transfer coefficient α and the exchange current density i_0 and is commonly known as the Tafel equation.

As discussed previously,[15] the anodic dissolution step (1) will always be very fast. This is because no crystallization overpotential is involved and also no concentration overpotential builds up due to the high electric field E. Hence, one can also exclude the anodic dissolution as the rate limiting process in our study. This leaves step (3), the electrocrystallization of Cu at the inert Pt electrode, as a most probable rate limiting step for the breakdown process.

Thus, from a physical point of view, the "ON resistance switching process" can be considered in the category of solid state transformations, such as crystallization from amorphous or glassy states, crystallographic changes, order-disorder changes and second-phase precipitation or dissolution processes.[33,34]

A solid state transformation such as metal electrocrystallization from a solid electrolyte, as in the present case, represents a first order phase transition involving the initial nucleation of Cu on the inert Pt electrode and the subsequent growth or electrodeposition of the metal phase.

Nucleation starts with the formation of unstable atom clusters (*embryos*). Some of the embryos shrink during this initial process while others eventually grow to reach a certain critical size beyond which they have a higher probability to grow than to dissolve, thus becoming a stable nucleus.[35,36] After a nucleus has attained its critical size, the transformation further proceeds by the growth of the product. The driving force for the nucleation and growth of the new metal phase is the supersaturation $\Delta\mu = ze\eta$. In general, the complete transformation phenomenon is controlled by a complex interplay of nucleation and growth.

In principle, for the case of resistive switching processes in electrochemical metallization cells, one can also expect a competition between a nucleation and a growth dominated filament formation. If the nucleation is relatively fast, the time needed to achieve breakdown or "ON resistance switching" could be identified with the time needed for the filament growth.[15] If the growth time is relatively fast, the switching time could be identified with the time required for the formation of a first critical Cu nucleus on the Pt electrode. In this case, the overall transformation time would be ruled by the nucleation rate. This implies that there might be two time scales associated with the switching process, and we speculate that these correspond to the nucleation process and the filament growth motion. The sum of these two time-scales represents the total switching time, i.e., nucleation time + growth time = total switching time. The interplay between these two processes makes it difficult to determine which process dominates the switching mechanism. Both will be discussed in detail in the following section.

IV. BASIC CONCEPTS OF NUCLEATION AND GROWTH

Before going ahead with the discussion on breakdown statistics, some basic concepts of nucleation theory, important for our analysis, are presented in this section. As mentioned above, the transformation starts with the formation of small, unstable nuclei of the new phase. Eventually, some nuclei reach a critical size beyond which they are stable.

Nucleation can preferably occur at random positions in the original phase (homogeneous nucleation) or at preferential sites like surfaces, interfaces, and lattice defects (heterogeneous nucleation). The classical thermodynamic treatment of phase stability by Gibbs provides the fundamentals of nucleation theory.[37] According to this theory, the formation of a new phase from the parent phase requires the creation of an interface between two phases, which requires work. Hence, there exists a free energy barrier to the formation of the new phase, which is given by the Gibbs free energy change ΔG for a closed system at constant volume and temperature. During the initial stage of nucleation, for small particles, the interfacial energy is much greater than the volume free energy in transforming to more stable nuclei. As the size of an embryonic nucleus increases, however, the interfacial energy becomes smaller with respect to the volume free energy and, at some critical size, the latter will predominate. The further accretion of atoms will then lead to the formation of a stable nucleus.

We consider now a cluster of N atoms which is formed on a substrate. The total Gibbs free energy change of the system associated with the formation of an embryonic nucleus with size N is[35]

$$\Delta G(N) = -Nze\eta + \Phi(N). \tag{4}$$

The first term in this equation is related to the transfer of N metal ions from the electrolyte to the electrode under the action of the overpotential η, whereas the second term is associated with the creation of new interfaces and is proportional to the surface area of the metal cluster. As illustrated schematically in Fig. 3, the $\Delta G(N)$ relationship displays a maximum at $N = N_{crit}$. The N_{crit} sized cluster is called critical nucleus and can grow spontaneously at the applied overpotential. The corresponding energy barrier $\Delta G(N_{crit}) \equiv \Delta G_{crit}$ represents the nucleation energy. According to the classical nucleation theory, $\Delta G(N_{crit})$ for the formation of 3D nuclei on an electrode surface is related to N_{crit} and η by[35,36]

$$\Delta G_{crit} = \frac{4B\sigma^3 V_m^2}{27(ze|\eta|)^2}, \tag{5a}$$

$$= \frac{N_{crit} ze|\eta|}{2}, \tag{5b}$$

where B is a geometrical factor depending on the shape of the critical 3D nucleus, σ represents the average specific surface energy of the nucleus and V_m is the volume of an atom in the nucleus.

According to classical nucleation theory, the stationary nucleation rate J, i.e., the number of stable nuclei which are formed per unit time per unit area is given by

$$J = J_0 \exp\left[-\frac{\Delta G_{crit}}{k_B T}\right], \tag{6}$$

where the preexponential factor J_0 is only a weak function of the overpotential and can be roughly treated as a constant.[35,36]

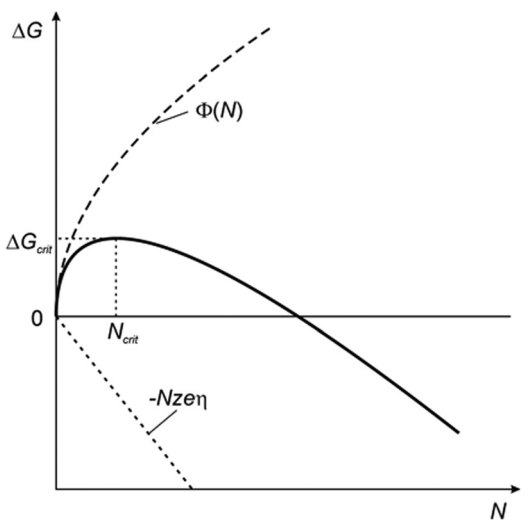

FIG. 3. Schematic representation of the work ΔG_{crit} required to nucleate a cap-shaped hemispherical nucleus of N_{crit} atoms on an electrode surface.

The corresponding average nucleation time τ_n is related to the stationary nucleation rate J and the inert electrode area A by $\tau_n = 1/JA$ and hence we have

$$\tau_n = \frac{1}{J_0 A}\exp\left[\frac{\Delta G_{crit}}{k_B T}\right]. \quad (7)$$

Using Eq. (5a), one obtains

$$\tau_n = \frac{1}{J_0 A}\exp\left[\frac{4B\sigma^3 V_m^2}{27(ze|\eta|)^2 k_B T}\right]. \quad (8)$$

Note, that Eq. (8) requires the validity of the treatment of the new phase as a continuum with bulk properties, known as the "classical approach." This condition is applicable only for relatively low overpotentials where the critical nucleus is sufficiently large. For higher overpotentials, the number of atoms which constitute the critical nucleus, N_{crit}, decreases drastically to only a few atoms, or even a single atom. Macroscopic quantities such as volume, surface, surface energy etc., lose their physical meaning; hence, the classical approach is no longer valid in this case and the use of an atomistic force interaction approach becomes more reasonable.

According to atomistic theory, N_{crit} remains constant in given overpotential intervals, so that in each of these intervals the corresponding overpotential dependence of the average nucleation time, τ_{na}, can be expressed by the equation[15,35]

$$\tau_{na} = K(Z_0, N_{crit})\exp\left[-\frac{(\alpha + N_{crit})ze}{k_B T}|\eta|\right], \quad (9)$$

where the preexponential term $K(Z_0,N_{crit})$ depends on N_{crit} and on the number density Z_0 of nucleation sites. In general, this preexponential factor involves overpotential and temperature dependent factors such as the Zeldovich factor and the attachment probability of the ions to the nucleus.[35,36] However, these dependencies can be disregarded in an analysis of experimental data if one is merely interested in an approximate estimation of the nucleation parameters.

As mentioned above, after a nucleus has attained its critical size, the breakdown processes further proceeds by the growth of a filament. Following Waser *et al.*,[15] the electrodeposition current density i is related to the normal growth rate R of the metal phase by Faraday's law $i = zeR/V_m$, where V_m is the atomic volume of the metal. Considering the one dimensional growth of a metal filament in our memory cells, the time τ_g for bridging both electrodes can be expressed as[15]

$$\tau_g = \frac{L}{R} = \frac{Lze}{V_m i}, \quad (10)$$

where L is the $Ge_{0.3}Se_{0.7}$ film thickness

Using Eq. (3a), one obtains

$$\tau_g = \frac{Lze}{V_m i_0}\exp\left[-\frac{\alpha ze}{k_B T}|\eta|\right]. \quad (11)$$

Note that both the average nucleation time, τ_{na}, and the growth time, τ_g, show an exponential dependence on overpotential and temperature [cf. Eqs. (9) and (11)]. At a first glance, it seems difficult to distinguish between these two processes. However, a comparison of the rate parameters, charge transfer coefficient α and $\xi = (\alpha + N_{crit})$, extracted from the slope of the $\ln(\tau_g)$ vs η and $\ln(\tau_{na})$ versus η plots, could make it feasible to differentiate between both. Charge transfer coefficient values lie in the range $0 < \alpha < 1$ and are typically ≈ 0.5 for direct charge transfer electrochemical reactions.[35] Hence, an extracted rate parameter value $\xi > 1$ might indicate nucleation as the rate limiting process rather than the growth of the filament. In such a case, from the slopes of the curves $\ln(\tau_n)$ vs $1/\eta^2$, $\ln(\tau_{na})$ vs η and $\ln(\tau_n)$ vs $1/T$, the respective nucleation rate parameters can be obtained to roughly estimate ΔG_{crit} and N_{crit}.

In the present study, we now assume that the first current jump observed in our breakdown measurements (cf. Fig. 2) corresponds to the time it takes to either form the first critical nuclei or to grow the bridging filament. As an illustration, the formation of a cap shaped hemispherical nucleus followed by a subsequent filament growth in Cu doped $Ge_{0.3}Se_{0.7}$ is depicted in Fig. 4. We have mentioned in chapter 2 that the "time-to-breakdown" seems to be a statistically distributed quantity. Thus, the probability that a given memory cell will switch within a given time interval from HRS to LRS under constant voltage stress conditions is the significant quantity. Then, within this context, the dependence of the breakdown probability distribution on external parameters such as voltage, thickness, temperature and area can be used to statistically analyze the breakdown phenomena within the framework of the nucleation and growth model.

V. RESULTS AND DISCUSSION

In general, the statistical distribution of time dependent failure processes which result from "weakest-link" type of effects or from physical processes that follow a Poisson distribution such as nucleation are typically described by means of the Weibull function,[23,38]

$$F(t) = 1 - \exp\left[-\left(t/\tau\right)^{\beta}\right]. \quad (12)$$

Here, F is the cumulative failure probability, t the time, τ the characteristic failure or breakdown time for $F = 0.63$ and β the slope parameter of the distribution. The slope parameter

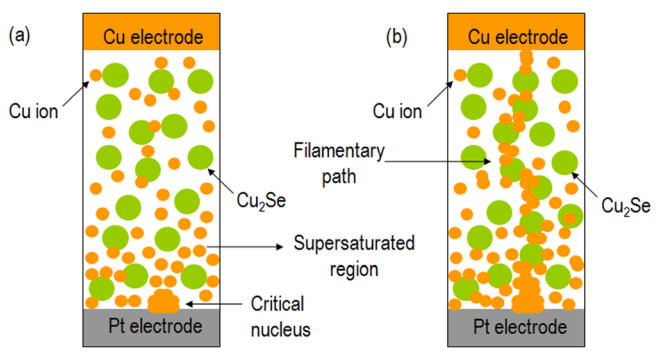

FIG. 4. (Color online) (a) Schematic illustration of a cap-shaped hemispherical nucleus formation in a $Ge_{0.3}Se_{0.7}$ memory cell. (b) A conductive filament formation that shorts the electrode.

represents the slope of a straight line which is obtained by plotting ln[-ln(1 - F)] for a Weibull distribution against ln(t).

As shown in Eqs. (8), (9), and (11), the natural logarithm of the average nucleation and growth times, τ_n, τ_{na}, and τ_g, depends inversely on both the overpotential η and the temperature T. Therefore, according to the nucleation and growth model, one would expect a significant decrease in τ_n, τ_{na}, and τ_g with increasing voltage and temperature. We now assume that the "time-to-breakdown," t_{BD}, when the first current jump or first prebreakdown event is observed on a memory cell under constant voltage stress can be identified as the time required to form the first critical nucleus or to grow the bridging filament. Thus, one should expect that the Weibull characteristic failure time τ will depend in the same manner on the overpotential and the temperature as τ_n, τ_{na}, and τ_g.

In our breakdown study, constant voltage stress measurements were performed at room temperature as well as at higher temperatures on planar capacitor structure dual-layered electrolytic memory cells integrated with different $Ge_{0.3}Se_{0.7}$ active layer thicknesses and a constant buffer layer thickness of ~2 nm. A maximum measurement time of 3600 s was set for all experiments and around 30 – 35 devices were used to arrive at the t_{BD} probability distributions at particular conditions. A current jump with a change of two orders of magnitude was specified as the failure criterion throughout the study.

A. Voltage dependence

Figure 5(a) shows Weibull plots of the cumulative t_{BD} probability distributions for memory cells with a $Ge_{0.3}Se_{0.7}$ active layer thickness of 90 nm and 50×50 μm^2 cross-sectional area, at different constant voltage stresses. All the corresponding breakdown experiments were performed at room temperature. The Weibull slope parameters were calculated by least-square fits of the cumulative t_{BD} probability distributions with a confidence level of 95%. They do not show any clear dependence on the applied voltage stress value in our study.

We found Weibull slope parameters of $\beta = 0.72$, 0.81, 1.05, 0.96, and 0.65 for constant voltage stresses of $V = 180$, 200, 220, 240, and 260 mV, respectively. The slope parameter is an important factor in reliability analysis. A low value of the slope parameter (<1) indicates more spread in the distribution, which is not desirable from an application point of view. The physical reasons for the observed $\beta < 1$ values are not fully understood yet, but these results might be attributed to film thickness non-uniformity and to some extent to the small number of devices used for estimating β values in this statistical study. Further studies including an area dependence analysis (as shown below) are needed to cross-check these discrepancies.

Despite the observed randomness in β, one clearly sees from Fig. 5(a) that the characteristic breakdown time τ, as expected, decreases with increasing voltage stress across the memory cells. Figure 5(b) depicts ln(τ) as a function of the applied voltage stress. Considering the overpotential η, as a first approximation, to be equal to the applied voltage stress V, the observed linear behavior of ln(τ) vs V indicates that our breakdown statistics is consistent with the critical nucleus formation or filament growth concept as expected from Eqns. (9) and (11). From the slope of the curve, we obtained

$$103.5 = \frac{\alpha z e}{k_B T}, \text{ growth model,} \tag{13a}$$

$$= \frac{\xi z e}{k_B T}, \text{ nucleation model.} \tag{13b}$$

With $T = 300$ K, one gets $\alpha \approx 2.7/z$. As mentioned earlier, in case of electrochemical reactions, the cathodic charge

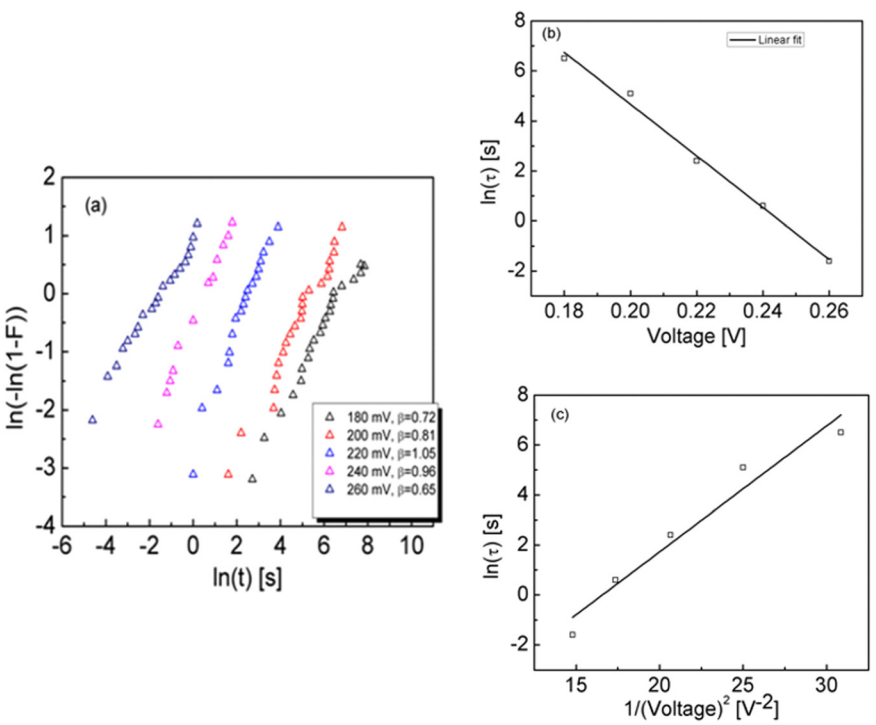

FIG. 5. (Color online) (a) Weibull plots of the cumulative "time-to-breakdown" distributions for memory cells with a 90 nm $Ge_{0.3}Se_{0.7}$ film at different constant voltage stresses. (b) ln(τ) vs V plot to ascertain nucleation rate parameters according to the atomistic nucleation model. (c) ln(τ) vs V^{-2} plot to ascertain nucleation rate parameters according to the classical nucleation model.

transfer coefficient lies always in the range $0 < \alpha < 1$. Even if we assume $z = 2$, we do not get any realistic value for α. We thus believe that the nucleation process rather than the filament growth process governs the characteristic breakdown time in our memory cells for the voltage range used in this study.

According to the atomistic nucleation model, we thus have $\xi = (\alpha + N_{crit}) = 2.7/z$. Using $\alpha \approx 0.5$ for the direct charge transfer case and $z = 1$, we find $N_{crit} \approx 2.2$, i.e., the critical nucleus consists of approximately 2–3 atoms in the voltage interval 0.18 – 0.26 V.

Next, we have used the classical nucleation model to roughly estimate the critical Gibbs nucleation energy, ΔG_{crit}, and critical nucleus size, N_{crit}. Figure 5(c) presents the experimental data for the characteristic breakdown time τ in a $\ln(\tau)$ vs $1/V^2$ plot. An analysis based on Eqs. (8), (5a), and (5b) shows that, in the studied voltage stress interval of 0.18 – 0.26 V, ΔG_{crit} varies between 0.40 and 0.19 eV, while N_{crit} varies between 4.4 and 1.5. It is important to point out that the number of atoms comprising the critical nucleus at 0.22 V, $N_{crit} \approx 2.1$, agrees well for both the classical and atomistic treatments. This indicates that both equations, the classical Eq. (8) and the atomistic Eq. (9), coincide in the high overpotential region, but that the value of N_{crit} is too small to make the classical treatment acceptable. However, going to lower overpotentials where the critical nucleus is sufficiently large, a classical representation could be more informative.[35,36]

Recently, Russo *et al.*[39] have studied the voltage dependence of the programming time for the "ON resistance switching" on a comparable system, Ag doped Ge-S (active layer thickness 60 nm). For applied cell voltages >0.4 V, they found a clear exponential decrease of the programming or switching time with increasing voltage. Based upon a fit of their experimental data and the resulting fit parameters, Russo *et al.*[39] suppose that at voltages >0.4 V the programming speed might be controlled by an electrochemical reaction like charge transfer or by ion migration processes. At voltages <0.4 V, however, considerable deviations were found (see Fig. 6 in Ref. 39) which could not simply be explained by a charge transfer or ion migration model. These findings might indicate that at lower applied voltages another process starts to dictate the overall switching behavior and it is reasonable to assume that nucleation processes might come into play. Generally, as the nucleation, charge transfer and ion migration rate have a different exponential dependence on the applied voltage, one can expect a transition from a charge transfer or ion migration to a nucleation controlled filament formation within a certain voltage range.

B. Temperature dependence

In the previous section, information about ΔG_{crit} and N_{crit} has been obtained from the voltage dependence of the characteristic breakdown time τ. As a test of the robustness of our nucleation model, these values have to be compared with results from the temperature dependence of the characteristic breakdown time.

Therefore, we have investigated the t_{BD} probability distributions under a constant voltage stress of 120 mV at different temperatures for 90 nm $Ge_{0.3}Se_{0.7}$ films integrated in planar structures with 50×50 μm^2 cross-sectional area. The Cu top electrode was covered with a 30 nm sputtered Pt film to prevent oxidation at higher temperatures. Figure 6(a) shows Weibull plots of the cumulative distributions of the measured t_{BD} for different temperatures. As expected, the characteristic time τ decreases with increasing temperature. ΔG_{crit} was calculated from the Arrhenius plot of $\ln(\tau)$ vs $1/T$ as shown in Fig. 6(b) and was found to be around 0.71 eV. Extrapolating to $V = 0.22$ V, one finds by means of Eq. 5(a) $\Delta G_{crit} = 0.71$ eV* $(0.12\ V)^2/(0.22\ V)^2 \approx 0.21$ eV, a value which is in good agreement with that calculated from the voltage dependence.

Using Eq. 5(b) with $\Delta G_{crit} = 0.71$ eV, $z = 1$ and $V = 0.12$ V, we assess N_{crit} to be approximately 12 atoms. In case the critical nucleus has the form of a hemisphere and considering that the atoms are closely packed, the diameter of this hemisphere will be around 1 nm. This calculated diameter of the critical nucleus might give a rough estimation of the minimum feature size of filaments formed in these memory cells during the prebreakdown process.

Thus, from the above discussion, at least for the voltage range used in this study, both the voltage and temperature dependence of the characteristic breakdown times and the derived values for the involved physical quantities strongly indicate that nucleation dominates the "ON resistance switching" speed. However, one can expect a crossover from nucleation to a growth rate limited switching within a certain voltage range varying for different material systems.

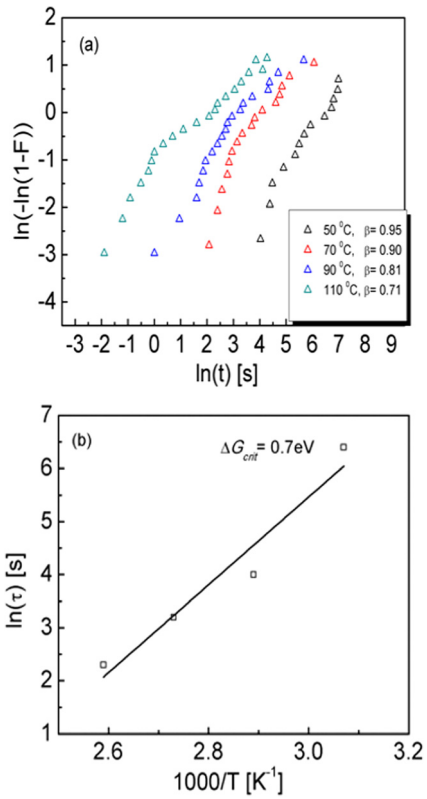

FIG. 6. (Color online) (a) Weibull plots of the cumulative "time-to-breakdown" distributions for memory cells with a 90 nm $Ge_{0.3}Se_{0.7}$ thin film at different temperatures (constant voltage stress: 120 mV). (b) The Arrhenius plot of $\ln(\tau)$ vs $1/T$.

C. Thickness dependence

The high scaling possibilities of RRAM based future non-volatile memories is one of the main driving forces behind the growing scientific and technological interests.[15] Though we have qualitatively estimated the size of the filament based on a nucleation model which is quite promising from the scalability point of view, it is still too early to predict the scalability of RRAM based memory devices as long as the various fundamental issues related to these memory devices such as underlying switching mechanism,[15] reliability[26] and noise properties[40] are not addressed thoroughly. In the literature, breakdown analysis is commonly used as a unique tool to investigate the scaling effects on device reliability and performance.[20–24] Hence, not only to verify the compatibility of the proposed nucleation model, but also from the device reliability point of view, it becomes important to investigate the thickness and area dependencies of the t_{BD} probability distributions on Cu doped $Ge_{0.3}Se_{0.7}$ solid electrolyte based memory devices.

Figure 7(a) shows Weibull plots of the cumulative t_{BD} probability distributions for $Ge_{0.3}Se_{0.7}$ films with thicknesses ranging from 30 to 120 nm. The measurements were performed at room temperature by applying a constant voltage stress of 180 mV on memory cells with 50×50 μm^2 cross-sectional area. As can be seen, the Weibull slope parameter β is approximately the same for memory devices with different thicknesses. The characteristic breakdown time increases exponentially with increasing the thickness of integrated $Ge_{0.3}Se_{0.7}$ thin film as shown in Fig. 7(b).

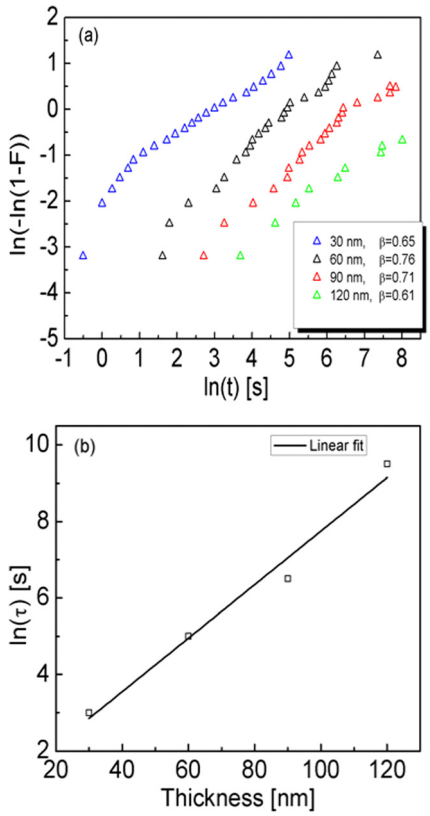

FIG. 7. (Color online) Weibull plots of the cumulative "time-to-breakdown" distributions for memory cells with different $Ge_{0.3}Se_{0.7}$ active layer thicknesses at room temperature (constant voltage stress:180 mV). (b) Exponential dependence of the characteristic breakdown time τ on the thickness of the integrated $Ge_{0.3}Se_{0.7}$ thin film.

Given that, based on the above discussion, the classical nucleation model accounts fairly well for the randomness observed in our breakdown study, one is then left with the question of a possible physical explanation for the dependence of the characteristic breakdown time on the integrated thickness of the active material. Though the exact physical explanation is yet not clear, there are some possible reasons for this observation.

On the one hand, one has to take into account that Cu doped $Ge_{0.3}Se_{0.7}$ is an inhomogeneous material system. As in the case of Ag doped Se-rich Ge_xSe_{1-x},[16] Cu doped $Ge_{0.3}Se_{0.7}$ probably consists of nanosized, mixed ionic-electronic conducting Cu_2Se precipitates which are separately dispersed in a continuous, high-resistivity Ge-rich Ge-Se matrix (cf. Fig. 4). Under polarizing conditions, the electric field will distribute in a complex manner inside the Cu doped Ge-Se film owing both to inhomogeneous local electronic and ionic conductivities and to the inner surfaces that can give rise to the build-up of space charge regions. It is thus reasonable to assume that the average voltage drop at the interface Pt cathode/electrolyte which establishes the overpotential might be only a fraction of the externally applied voltage. In case this fraction decreases with increasing film thickness, one would expect some exponential dependence of the characteristic breakdown time on film thickness. Under this point of view, the values for the critical nucleus size as determined in sections (A) and (B) should be regarded as minimum limiting values.

On the other hand, we believe that direct electric field effects on the nucleation process could be another possible reason for the observed thickness dependence. This is particularly important in case of thin film material systems, such as our memory devices, where the strong electric field across the memory cell could significantly influence the nucleation process and, hence, the resistive switching process. The high electric field E across the growing nucleus, in addition to the applied overpotential, could further increase the nucleation probability by suppressing the nucleation barrier through the decrease in the electrostatic energy F_E and could thus contribute significantly to the free energy change for the formation of stable nuclei. Considering the electric field effect, Eq. (4) can be generalized as

$$\Delta G(N) = -Nze\eta + \Phi(N) + F_E. \tag{14}$$

Field induced nucleation becomes dominant when the decrease in $\Delta G(N)$ owing to F_E exceeds the contribution of the supersaturation. Following the approach of the high field induced nucleation model for threshold switching behavior in PCRAM, as proposed by Kaprov *et al.*,[41,42] the nucleation time varies as

$$\tau_E \sim \exp\left[\frac{(\Delta G_{crit})_0}{k_B T}\frac{E_0}{E}\right], \tag{15}$$

where $(\Delta G_{crit})_0$ is the classical critical Gibbs nucleation energy and E_0 is a characteristic electric field. E should be

approximately related to the external voltage V and film thickness L such as $E \sim V/L$.

In principle, this model explains very well the observed exponential dependence of the characteristic breakdown time on the thickness of integrated $Ge_{0.3}Se_{0.7}$ thin film, as shown in Fig. 7(b). However, we know that $(\Delta G_{crit})_0$ itself depends on the overpotential. Therefore, within this model, it becomes difficult to distinguish between an electric field and overpotential dominated nucleation on base of the data presented. Further analysis at low electric field strengths could shed more light to make a distinction between these two regimes.

D. Area dependence

As shown above, nucleation and thus the ensuing breakdown events obey a statistical distribution which can be analyzed according to Weibull statistics. One property of the Weibull function F is that F should scale with the electrode area A of the devices if the nucleation sites are randomly distributed on the electrode:[23]

$$\ln[-\ln(1-F')] - \ln[-\ln(1-F)] = \ln\left(\frac{A'}{A}\right). \quad (16)$$

From this equation it follows that if the area is increased by a factor (A'/A) then the t_{BD} probability distribution shifts vertically by $\ln(A'/A)$ along the Weibull scale and the characteristics time τ decreases to τ', according to[23]

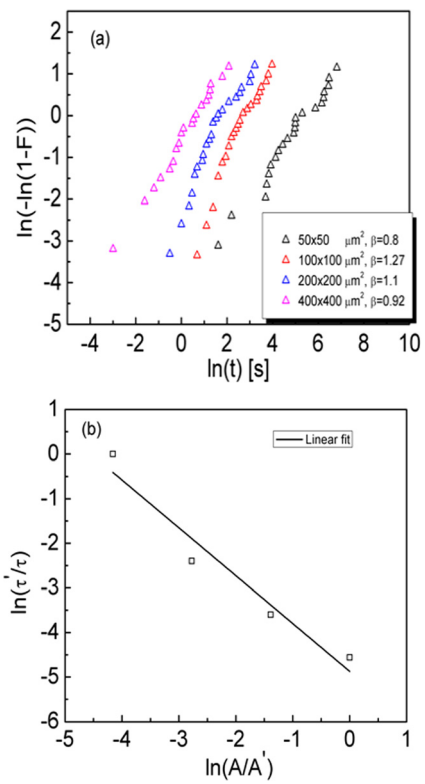

FIG. 8. (Color online) (a) Weibull plots of the cumulative "time-to-breakdown" distributions for memory cells with different cross-sectional areas and a 90 nm $Ge_{0.3}Se_{0.7}$ thin film at room temperature (constant voltage stress: 200 mV). (b) The normalized characteristic breakdown time $\ln(\tau'/\tau)$ as a function of the normalized memory devices cross-sectional area $\ln(A/A')$.

$$\frac{\tau'}{\tau} = \left(\frac{A}{A'}\right)^{\frac{1}{\beta}}. \quad (17)$$

By measuring the t_{BD} distribution functions on devices with different areas, one can verify whether the nucleation sites are randomly distributed. To check this property, we investigated the influence of the memory device cross-sectional area on the t_{BD} probability distributions. The measurements were performed at room temperature under a constant voltage stress of 200 mV on memory devices with a 90 nm $Ge_{0.3}Se_{0.7}$ film. Figure 8(a) shows the cumulative t_{BD} distribution for different electrode areas ranging from 50×50 to 400×400 μm^2. As can be seen, there is a clear shift vertically along the Weibull scale with increasing device area. Further, the power law dependence of τ on area [Eq. (17)] can be used to extract a more exact value for the slope parameter β rather than using a linear fit of a single Weibull distribution. Figure 8(b) shows the linear dependence of $\ln(\tau'/\tau)$ on $\ln(A/A')$ according to Eq. (17). The calculated value of β is found to be $\sim$1, which indicates that the breakdown process in our memory cells is of intrinsic nature. Indeed, in the future, this approach has to be followed to carefully cross-check the observed randomness of the Weibull slope parameters as found in the present breakdown study on $Ge_{0.3}Se_{0.7}$ based memory cells.

VI. CONCLUSIONS

In summary, the "ON resistance switching" statistics was studied to understand the stochastic nature of the resistance switching behavior of Cu doped $Ge_{0.3}Se_{0.7}$ based memory devices. Based upon an analysis of the voltage and temperature dependence of the characteristic switching time, the observed switching statistics was found to be related to the stochastic nature of underlying nucleation processes which induce the formation of the conducting filament. For the voltage range used in this study, we obtained a critical Gibbs nucleation energy in the range 0.71 −0.22 eV, corresponding to a number of atoms forming the critical nucleus in the range 12 – 2.3. A linear dependence of the characteristic breakdown time on the film thickness probably indicates that an electric field effect needs to be considered in addition to overpotential driven nucleation.

At the end, though our breakdown analysis on Cu doped $Ge_{0.3}Se_{0.7}$ based memory cells indicates that "ON resistance switching" is governed by nucleation effects, yet there are some critical points which need to be considered in future to improve our understanding. First, the influence of the disorder on nucleation and, hence, on the fluctuations in device performance is not included in the proposed model. To be precise, disorder can come into play in many ways during the resistive switching process. The switching process enhances an initially present disorder through the nucleation of new local conductive paths and branches or, simply, due to the heterogeneity of the electric field stress that results from the complex geometrical rearrangement of existing local conductive paths. Even a small initially present disorder in the material systems can be enormously amplified during switching. Additionally, the enormous statistical

fluctuations in the electrical field in disordered material systems could easily lead to enormous statistical fluctuations in the time required for "ON resistance switching."

Second, in our analysis, we have not considered the lateral growth of the filament after the first prebreakdown event (see Fig. 2), the dynamics of which could be important for a further understanding of the retention behavior of these memory cells.

Third, for industrial applications, these memory devices should display fast (ns-scale) writing speed. In this time scale, all the processes discussed above, i.e., ion migration, nucleation and filament growth, could play an essential role in the switching behavior. Hence, it becomes important to distinguish between the rate limiting processes for reliable and fast switching memory devices.

Finally, although the approach used in this article provides a route to understand the stochastic nature of the resistive switching behavior, the above mentioned critical points highlight some of the challenges ahead for developing reliable RRAM based memory devices for future applications.

[1]T. W. Hickmott, J. Appl. Phys. **33**, 2669 (1962).
[2]J. F. Gibbons and W. E. Beadle, Solid-State Electron. **7**, 785 (1964).
[3]E. L. Cook, J. Appl. Phys. **41**, 551 (1970).
[4]F. A. S. Al-Ramadhan and C. A. Hogarth, J. Mater. Sci. **19**, 1939. (1984).
[5]A. Beck, J. G. Bednorz, Ch. Gerber, C. Rossel, and D. Widmer, J. Appl. Phys. **77**, 139 (2000).
[6]C. Rossel, G. I. Meijer, D. Brémaud, and D. Widmer, J. Appl. Phys. **90**, 2892 (2001).
[7]A. Baikalov, Y. Q. Wang, B. Shen, B. Lorenz, S. Tsui, Y. Y. Sun, Y. Y. Xue, and C. W. Chu, Appl. Phys. Lett. **83**, 957 (2003).
[8]K. Szot, W. Speier, G. Bihlmayer, and R. Waser, Nature Mater. **5**, 312 (2006).
[9]G. Dearnaley, A. M. Stoneham, and D. V. Morgan, Rep. Prog. Phys. **33**, 1129 (1970).
[10]D. P. Oxely, Electrocomponent Sci. Technol. **3**, 217 (1977).
[11]H. Pagnia and N. Sotnik, Phys. Status Solidi A **108**, 11 (1988).
[12]Y. Watanabe, Ferroelectrics **349**, 190 (2007).
[13]R. Waser and M. Aono, Nature Mater. **6**, 833 (2007).
[14]S. F. Karg, G. I Meijer, J. G. Bednorz, C. T. Rettner, A. G. Schrott, E. A. Joseph, C. H. Lam, M. Janousch, U. Staub, F. La Mattina, S. F. Alvarado, D. Widmer, R. Stutz, U. Drechsler, and D. Caimi, IBM J. Res. Dev. **52**, 481 (2008).
[15]R. Waser, R. Dittmann, G. Staikov, and K. Szot, Adv. Mater. **21**, 2632 (2009).
[16]M. N. Kozicki, M. Park, and M. Mitkova, IEEE Trans. Nanotechnol. **4**, 331 (2005).
[17]M. N. Kozicki, M. Balakrishan, C. Gopalan, C. Ratnakumar, and M. Mitkova, *Proceedings of IEEE Non-Volatile Memory Technology Symposium* (IEEE, New York, 2005), Vol. 83.
[18]Z. Wang, P. B. Griffin, J. McVittie, S. Wong, P. C. McIntyre, and Y. Nishi, IEEE Electron Device Lett. **28**, 14 (2007).
[19]C. Schindler, M. Weides, M. N. Kozicki, and R. Waser, Appl. Phys. Lett. **92**, 122910 (2008).
[20]J. S. Suehle, IEEE Trans. Electron Devices **49**, 6 (2002).
[21]J. H. Stathis and S. Zafar, Microelectron. Reliab. **46**, 270 (2006).
[22]G. Ribes, J. Mitard, M. Denais, S. Bruyere, F. Monsieur, C. Parthasarathy, E. Vincent, and G. Ghibaudo, IEEE Trans. Electron Devices Mater. Reliab. **5**, 1 (2005).
[23]J. H. Stathis, J. Appl. Phys. **86**, 5757 (1999).
[24]J. Das, R. Degraeve, G. Groeseneken, S. Stein, H. Kohlstedt, G. Borghs, and J. De Boeck, J. Appl. Phys. **94**, 2749 (2003).
[25]C. P. McHardy, A. G. Fitzgerald, P. A. Moir, and M. Flynn, J. Phys. C **20**, 4055 (1987).
[26]R. Soni, M. Meier, A. Rüdiger, B. Holländer, C. Kügeler, and R. Waser, Microelectron. Eng. **86**, 1054 (2009).
[27]R. Soni, P. Meuffels, H. Kohlstedt, C. Kügeler, and R. Waser, Appl. Phys. Lett. **94**, 123503 (2009).
[28]I. Zvyagin, in *Charge Transport in Disordered Solids with Applications in Electronics*, edited by Sergei Baranovski (John Wiley and Sons, Ltd., Chichester, England, 2006), Chap. 9.
[29]N. F. Mott and R. W. Gurney, *Electronic Processes in Ionic Crystals* (Oxford University Press, Oxford, 1948).
[30]J. J. O'Dwyer, *The Theory of Electrical Conduction and Breakdown in Solid Dielectrics* (Clarendon, Oxford, 1973).
[31]D. N. Tafen, D. A. Drabold, and M. Mitkova, Phys. Rev. B **72**, 054206 (2005).
[32]A. Bard and L. Faulkner, *Electrochemical Methods: Fundamentals and Applications* (Wiley, New York, 2001).
[33]J. W. P. Schmelzer, *Nucleation Theory and Applications* (Wiley-VCH, Berlin, 2005).
[34]H. E. Stanley, *Introduction of Phase Transitions and Critical Phenomena* (Clarendon, Oxford, 1971).
[35]E. Budevski, G. Staikov, and W. J. Lorenz, *Electrochemical Phase Formation and Growth* (VCH Verlagsgesellschaft mbH, Weinheim, 1996).
[36]A. Milchev, *Electrocrystallization: Fundamentals of Nucleation and Growth* (Kluwer Academic Publishers, Dordrecht, 2002).
[37]J. W. Gibbs, *Collected Works*, Vol. 1 (Longmans, Green, New York, 1948).
[38]W. Weibull, J. Appl. Mech. **18**, 293 (1951).
[39]U. Russo, D. Kamalanathan, D. Ielmini, A. L. Lacatia, and M. N. Kozicki, IEEE Trans. Electron Devices **56**, 1040 (2009).
[40]R. Soni, P. Meuffels, A. Petraru, M. Weides, C. Kügeler, R. Waser, and H. Kohlstedt, J. Appl. Phys. **107**, 024517 (2010).
[41]V. G. Karpov, Y. A. Kryukov, I. V. Karpov, and M. Mitra, Phys. Rev. B **78**, 052201 (2008).
[42]V. G. Karpov, Y. A. Kryukov, M. Mitra, and I. V. Karpov, J. Appl. Phys. **104**, 054507 (2008).